Lead Article

J. Synchrotron Rad. (1996). **3**, 250–259

Recording Diffraction Data for Structure Determination for Very Small Crystals

Marjorie M. Harding

Department of Chemistry, University of Liverpool, PO Box 147, Liverpool L69 3BX, UK. E-mail: mmh@liv.ac.uk

(*Received 7 May 1996; accepted 27 June 1996*)

An account is given of experiences in recording diffraction data with synchrotron radiation to determine structures for very small crystals, too small for use with conventional X-ray sources and diffractometers. The effect of crystal composition as well as size on the relative intensity of diffraction patterns of different crystals is noted. Crystal mounting is briefly described. Experimental methods are outlined including detectors and other instrumentation, and a range of examples is given; these include the use of both monochromatic area-detector systems for intensity measurement and of the white-beam Laue method. Choice of the shortest wavelength available with adequate intensity is recommended. The examples include organic, organometallic and aluminophosphate compounds; in all cases structure determination was important in relation to chemical research projects – they were not chosen as 'test' crystals. Comparison is made of the quality of the structure refinements achieved with those from synchrotron radiation powder diffraction – the alternative method when good-sized crystals are not available. Commonly it is found that when good-quality large crystals of a substance cannot be grown, the small crystals are poor in quality with substantial mosaic spread; the relationship between mosaic spread, structure, morphology and crystal growth is explored.

Keywords: small crystals; structure determination; mosaic spread; crystal quality.

1. Introduction

This is an account of experiences in attempting to record diffraction data with synchrotron radiation and to determine structures for very small crystals, too small for use with conventional X-ray generators and diffractometers. The application has been to a wide variety of real chemical problems which were presented, rather than systematic trials on test compounds whose structures were already known. It is almost entirely based on work done in my own research group, but a few examples of the work of others are used. Work with proteins is not included, although the weakness of the diffraction patterns for many protein crystals is comparable with those of the crystals discussed here; much of the instrumentation was developed primarily for protein crystallography (see Helliwell, 1992) and it has been possible to learn much from these techniques. Most of this work was completed before the advent of third-generation synchrotron sources, and these, together with new instrumentation, will allow much further development in the near future.

What are the challenges or likely areas of difficulty in recording data for such crystals ? It will be useful to consider how crystals can be mounted, whether radiation damage can be avoided, the prevalence of stacking faults or other crystal quality problems in small crystals, and means for achieving a satisfactory signal-to-noise ratio. In my experience in attempting to look at smaller and smaller crystals, the limit has been set by the last of these, *i.e.* the problem of measuring weak diffraction spots in the presence of a substantial background.

After a marvellous introduction to crystallography and structural chemistry in Professor Dorothy Hodgkin's laboratory in Oxford (1956–1962), Marjorie Harding moved to Edinburgh and worked on the structures of amino acids, their metal complexes, and two proteins. In 1980 she found herself in Liverpool (where her husband had moved to a new post); the time and the location (near Daresbury Laboratory) were good to begin exploring the use of synchrotron radiation for small crystals and for other applications in structural chemistry.

2. How small is small?

We need to consider the effect of crystal size, composition, wavelength and other factors on the intensity of the diffraction pattern to be measured. The average intensity of diffracted beams from a crystal is proportional to

$$\lambda^3 = LI_{\text{incident}}\langle|F(hkl)|^2\rangle V_{\text{crystal}}/V_{\text{cell}}^2,$$

where L is the Lorentz factor. Absorption effects are ignored here, and since the Lorentz factor is usually

approximately proportional to $1/\sin\theta$, and thus to $1/\lambda$, the average intensity is effectively dependent on λ^2. For crystals other than very simple ones, such as CaF_2, $KTiO_3$ *etc.*, replacement of $\langle|F(hkl)|^2\rangle$ by Σf^2 is a useful rough approximation; the summation is over all the atoms in the unit cell. (For more precise comparisons, values of Σf^2 at different $\sin\theta/\lambda$ and appropriately corrected for thermal vibration could be used.) If the crystal lattice is centred, and the summation is over the whole cell of volume V_{cell}, the average diffracted intensity calculated will be for all reflections including systematically absent ones; it is more helpful to use V_{cell} and Σf^2 for the primitive cell, in which case the average intensity will correspond to the observable reflections only.

Thus, for crystals of different sizes and compositions studied with the same X-ray source at the same wavelength, we need to compare

$$\Sigma f^2 \; V_{crystal}/V_{cell}^2 .$$

Table 1 gives some examples of different crystals which by this criterion should give diffraction patterns of the same average intensity, and they are all near the current lower limit for recording adequate diffraction data. It is clear that, apart from problems of mounting, the minimum size for a crystal whose diffraction pattern can be usefully recorded with a particular source and detector depends on its composition and its structure.

Table 1
Examples to show the effect of composition, space group and crystal volume on the average intensity to be expected in crystal diffraction patterns.

This can be roughly estimated as $V_{crystal} \times \Sigma f^2/V_{cell}^2$, and should be the same for all the five samples below. Fuller details of all but the last two are given in Table 2.

	Space group	Z	Crystal size (μm^3)
cdc: $C_{24}H_{40}O_4$	$P6_5$	6	48^3
VPI-5: $Al_3(PO_4)_3.5H_2O$	$P6_3$	6	27^3
$AlPO_4$-CHA: $Al_3(PO_4)_3$	$P\bar{1}$	2	17^3
$Cu_2(OH)_2CO_3$	$P2_1/a$	4	11^3
$PbCO_3$	$Pmcm$	4	5^3
Protein insulin (C_{256})	$R3$	6	150^3

3. Mounting of small crystals

As the scattering power of the crystal is very small, it is important to minimize the scattering effects of all mounting materials since this will contribute to the background. Fig. 1 illustrates the method we have used; the strand of glass wool (*ca* 10 μm thick) needs to be just long enough to keep the stouter glass fibre out of the X-ray beam, but otherwise as short as possible for mechanical stability. Crystals down to 5 μm in size have been mounted this way in our laboratory using a good microscope and a steady hand! Micromanipulators could be set up to help. Selecting a good crystal can be difficult when, as is often the case, the magnification of the microscope is not sufficient to assess the optical quality of the crystal or to observe faces or extinction effects satisfactorily. It may be necessary to examine the diffraction patterns of a number of crystals from a sample to select a satisfactory one.

4. Sources and detectors, outline of experimental methods

Discrimination of the signal from the noise when the diffraction pattern of the small crystal is recorded is the biggest challenge. Using conventional sources and diffractometers this can be improved to some extent by using longer counting times, but the time becomes prohibitively long, *e.g.* weeks or months. Increased source intensity can clearly help; rotating-anode generators can give very significant improvements, and a synchrotron source is better still. Further improvement will usually result from using an area detector, *i.e.* electronic, multiwire, image plate or CCD, rather than a scintillation counter recording reflections one at a time. For crystals of intermediate size, a rotating-anode system with area detector may well be an effective combination, but for the smallest crystals a synchrotron source will be needed, and has additional advantages. An account of beamline optics and instrumentation for single (protein) crystal data collection with synchrotron radiation is given by Helliwell (1992). The new materials science beamline at the ESRF (European Synchrotron Radiation Facility) is described by Krumrey, Kvick & Schwegle (1995).

The very low beam divergence of the synchrotron radiation beams often used (*e.g.* ≤ 1 mrad horizontally, ≤ 0.2 mrad vertically) should lead to small sharp diffraction spots, by comparison with those from typical sealed X-ray tube sources; they can be better discriminated from background and more accurately integrated. Many very small crystals show high mosaic spread (see §9) and for these the small beam divergence of a synchrotron source is doubly advantageous.

4.1. *Monochromatized synchrotron radiation*

Monochromatized synchrotron radiation has been used with a four- or five-circle diffractometer with scintillation counter, for example at Brookhaven National Labora-

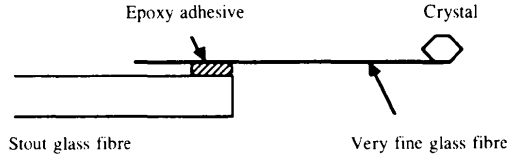

Figure 1
Mounting of a very small crystal. For mechanical stability the fine glass fibre should not be more than 0.2–0.3 mm in length beyond the end of the stout fibre. Strands of glass wool *ca* 10 μm in width have been used. The crystal is glued to the fine fibre with epoxy-resin thinned with 2-methoxyethanol.

tory, USA (King, Mundi, Strohmaier & Haushalter, 1991) and Hasylab, Germany (Lehmann *et al.*, 1990; Kohlmann, Sowa, Reithmayer & Schulz, 1994); individual reflections are counted one at a time. Small sharp reflections can be difficult to find, especially when they are sparse (small unit cell), thus the initial finding of unit cell and orientation is often slow. Thereafter, measurement is straightforward, following conventional patterns, except that the incident beam must be continuously monitored and its slowly diminishing intensity allowed for in the data processing.

Much of our work has used monochromatic synchrotron radiation with an Enraf–Nonius FAST detector – an electronic area-detector diffractometer – on SRS workstation 9.6 at Daresbury Laboratory. The beamline optics and workstation are described by Helliwell *et al.* (1986). The FAST detector is a TV-type detector which employs a prestorage-gain element/image intensifier [see Arndt, 1990; for other types of solid-state area detectors see the review of Allinson (1994)]. The FAST detector, 48 × 64 mm, 512 × 512 pixels, could be positioned at distances ≥ 40 mm from the crystal, and with its normal at an angle up to 28° from the incident beam direction. The crystal was rotated around φ on the goniostat and images or 'frames' were recorded for small angular ranges such as 0.4°, within times such as 20 s. With a wavelength of 0.90 Å this allows an almost complete hemisphere of the reciprocal lattice to be recorded in 450 frames. Normal to the rotation axis, the resolution is *ca* 0.85 Å, but data are missing from the cusp region around the rotation axis; additional frames with a different crystal orientation may be recorded to cover this. Typical data collections for small crystals (see examples in §7) took 2–10 h. Data processing requires the integration of the intensities in three-dimensional 'shoe boxes'; each spot must be integrated with respect to the reciprocal lattice coordinates ξ and ζ, and the spindle rotation φ, and this is achieved using the program *MADNES* (Messerschmidt & Pflugrath, 1987). Such three-dimensional integration should in principle give the best discrimination of spot over background – better than two-dimensional integration as in image-plate systems (below) or one-dimensional integration (ω or $\omega/2\theta$ scans) on a conventional diffractometer.

Image-plate systems are now frequently used for intensity measurements of protein crystals (see, for example, Helliwell, Ealick, Doing, Irving & Szebenyi, 1993) and should be suitable for small crystals. The high sensitivity, wide dynamic range and large dimensions (*e.g.* 25 cm or greater) are clear advantages. The pixel size for image-plate scanners is usually quite large (88, 100 μm or greater). Readout times are substantial (*e.g.* 2–10 min), so data collection is normally by a series of images at adjacent spindle angles, with an oscillation range which is the largest compatible with the avoidance of spot overlap; this might be 2–5° or more. Data processing now requires the integration of intensities in two dimensions on each image; spots whose angular range, φ, overlaps the end of one oscillation range and the beginning of the next will be classified as 'partials' on each range (and small crystals with large mosaic spread give a higher than normal proportion of such partial reflections).

CCD detectors (detectors with a phosphor, whose output is transmitted to a charge-coupled device for detecting the emitted light) have recently been introduced and hold considerable promise; the readout time is very much shorter, although the area covered is much smaller, than for an image plate (see, for example, Deacon *et al.*, 1995). The recording of monochromatic synchrotron radiation diffraction data for small crystals with such a detector will be attempted shortly (Flaherty *et al.*, 1995).

In all these area-detector methods the initial location of diffraction spots for cell and orientation determination is easier than with a single-counter diffractometer. The integration of intensity is potentially more accurate since it is two- or three-dimensional. There is a further important advantage. As it is normally possible to view the image during data collection it is immediately apparent if there are crystal quality problems, giving, for example, very streaked spots; such problems are very common with small crystals (see §9).

4.2. *The Laue method*

The Laue method can use most or all of the full 'white' beam of synchrotron radiation. Images such as that in Fig. 2 are recorded from a stationary crystal in milliseconds or seconds and a small number of images recorded with the crystal in different orientations (1–6, depending on crystal symmetry) is sufficient to include 80–95% of the unique reflections. Descriptions of the method are given by Harding (1995), Helliwell (1992), Helliwell *et al.* (1989), and an example of a complete structure determination by Dodd, Hao, Harding & Prince (1994). With normal-sized crystals, reflection intensities can be evaluated just about as accurately as by monochromatic methods for those reflections (*ca* 80% of the total) which are recorded as single reflection spots. A small proportion of the spots in the Laue diffraction pattern correspond to the superposition of the reflections *nh*, *nk*, *nl* for several integer values of *n*; deconvolution of these multiples yields useful estimates of the individual reflection intensities, but with presently available methods average errors, indicated by $R_{\rm merge}$ or $R_{\rm int}$, are about twice as great as for the single reflections. Film was used as detector in much of the development of the synchrotron radiation Laue diffraction method on account of its small pixel size; image plates are now used (Snell *et al.*, 1995) and CCD detectors. The unit-cell dimensions are not normally derivable from a Laue diffraction pattern. The axial ratios and angles can be derived (Carr, Cruickshank & Harding, 1992) and the cell dimensions can be determined if the minimum wavelength present in the incident synchrotron radiation beam is known exactly (Carr, Dodd & Harding, 1993).

For very small crystals the Laue method has the advantage of much shorter data collection times than any monochromatic method. However, discrimination of spot from background is not so good; the spot, integrated

in two dimensions on the detector, corresponds to one wavelength of the incident beam, but the background overlaid on it results from the scattering by fibre, air *etc.* of *all* the wavelengths present in the beam. The geometry of Laue diffraction is very sensitive to crystal quality; extended spots result from crystals with significant mosaic spread, and integration to give intensities can become impracticable.

5. Choice of wavelength or wavelength range

Although stronger diffraction patterns are obtained with longer wavelengths (§2), it will usually be best for monochromatic experiments to choose the shortest wavelength at which the diffraction pattern can be adequately detected. This reduces absorption and extinction effects, and very often also radiation damage. Most of our experiments used SRS workstation 9.6 with $\lambda = 0.90$ Å; $\lambda = 0.5$–0.6 Å or even less is conveniently available at some third-generation synchrotron sources. At short wavelengths, $2\theta_{max}$ for data to a given resolution is smaller; this can be helpful when the detector is small in area (typical with current CCD detectors), provided the diffraction spots are adequately resolved. For example, with the FAST diffractometer at its shortest crystal–detector distance, *ca* 40 mm, and maximum detector tilt, 28°, a wavelength of 0.9 Å gave data to *ca* 0.85 Å resolution; if a shorter wavelength had been available it would have allowed higher resolution data to be recorded (if the crystal diffracted well) and better structure refinement.

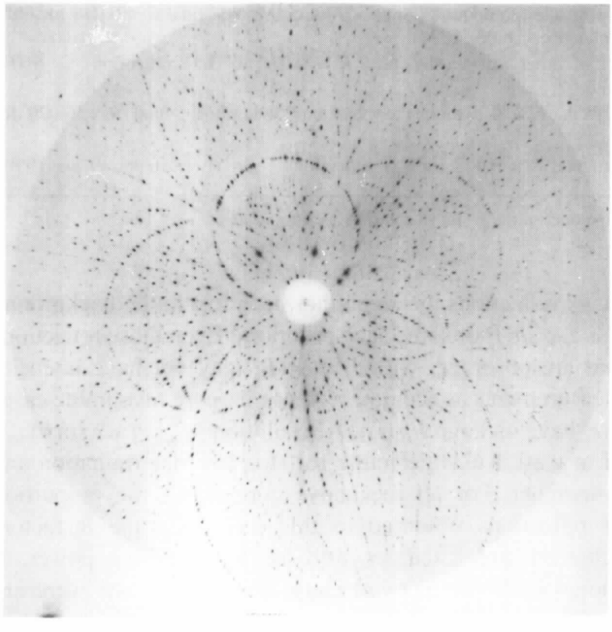

Figure 2
Laue diffraction pattern of a lanthanum complex, $La_3L(OH)_2(NO_3)_4.7H_2O$, where L is a macrocyclic ligand, $C_{36}H_{42}N_9O_3$. The image was recorded on film at Daresbury Laboratory, workstation 9.7; crystal–film distance 57 mm, exposure 0.2 s with 0.2 mm Al attenuator in beam.

The same principles apply in white-beam experiments. Radiation damage is a much greater risk, and it usually appears as increased mosaic spread, *i.e.* increased size of the diffraction spots on the detector, accompanied by decrease in intensity. The distribution of incident intensity with respect to wavelength is determined by the synchrotron source characteristics, and any optical elements in the beamline, but it can be modified by the insertion of absorbers, for example Al or Cu foils (see, for example, Harding, 1991). Alternatively, a long-wavelength cut-off can be achieved by glancing-angle reflection from a mylar film (Cassetta *et al.*, 1993). The complete removal of radiation with wavelengths > 1.2–1.4 Å can greatly reduce radiation damage in sensitive crystals, *e.g.* proteins, organic and organometallic compounds. The optimum wavelength range for a white-beam experiment also depends on the type of crystal under study, the maximum resolution (minimum d spacing) to which it can be expected to diffract, and the geometry of the detector (dimensions, distance from crystal, whether flat). The workstations developed at Daresbury Laboratory (9.5, 9.7), with flat film or image plates, give good data for proteins (d_{min} *ca* 2 Å) when the effective wavelength range is *ca* 0.5–1.5 or 2 Å (on station 9.5 radiation with wavelength less than *ca* 0.45 Å is removed by the focusing mirror system). For crystals of simpler compounds, with d_{min} 0.75–1 Å, a wavelength range of 0.25–0.75 or 1 Å (available only on 9.7) is much more effective for capturing a large proportion of data in a small number of images; this is because of the maximum θ imposed by the experimental geometry and/or the difficulties in measuring reflections with high θ which are incident very obliquely on the detector.

6. Reducing background scattering

In a good experimental arrangement the background above which the diffraction spots must be measured will be as low as possible, and will be due entirely to scattering by fibre, crystal, adhesive and air in the short beam path between the tip of the collimator and the backstop. In our experiments the collimator has usually been 0.15–0.20 mm in diameter, and in white-beam experiments, where the background problem is most critical, the collimator-to-backstop distance was less than 7–10 mm; this was made possible by a small carefully aligned backstop, *ca* 1 mm in diameter. Finer collimators are obviously highly desirable, but will require greater mechanical accuracy in the alignment of goniostat axes and collimator.

7. Examples

A number of examples of successful structure determinations are listed and compared in Table 2. These include (*a*) monochromatic recording of data with the FAST diffractometer, (*b*) data recorded with the full white beam by the Laue method, and (*c*) monochromatic recording of data using four- or five-circle diffractometers. (*a*) and (*b*) are

Table 2
Examples of structure determinations with small crystals.

Crystal	Space group	Unit cell volume (Å^3)	Scattering power $\Sigma f^2/V_{cell}^2$ (e^2 Å^{-6})	Crystal dimensions (μm)	Crystal volume × scattering power (× 10^{12} e^2 Å^{-3})	d_{min} for reported data (Å)	Fraction unique reflections to d_{min} = 1.0 Å
(*a*) Monochromatic data recorded with FAST diffractometer							
(1) Au_{10} cluster	P† ($C2/c$)	13246	0.0016	30 × 10 × 10	4.8	1.0	0.27 > 3$\sigma(I)$
(2) VPI-5	$P6_3$	2526	0.0021	70 × 10 × 10	15	1.0	0.55 > 2$\sigma(I)$
(3) $AlPO_4$-CHA	$P\bar{1}$	765	0.0079	35 × 20 × 15	83	1.0	0.18 > 2$\sigma(I)$
(4) Chenodeoxycholic acid (cdc)	$P6_5$	4397	0.00036	60 × 40 × 200	173	1.2	0.32 > 2$\sigma(F)$
(5) Aurichalcite	$P2_1/m$	461	0.0476	100 × 40 × 5	952	1.0	0.77 > 2$\sigma(I)$
(*b*) White-beam data recorded by Laue method							
(6) $Cu_2(OH)_2CO_3$	$P2_1/a$	389	0.027	20 × 20 × 10	108	0.9	0.38 > 2$\sigma(I)$
(7) Molybdophosphate	$P2_1/n$	5775	0.0015	100 × 140 × 15	316	1.05	0.47 > 4$\sigma(F)$
(8) Organic pigment	$P2_1/c$	1270	0.0041	160 × 20 × 30	397	0.84	0.74 > 4$\sigma(F)$
(9) Rh_2-organometallic	$P2_1/a$	6958	0.00068	200 × 200 × 20	547	1.0	0.49 > 2$\sigma(I)$
(*c*) Other							
(10) YPO_4	P† ($I2/a$)	232	0.079	113 × 5 × 4	179	0.70	2.6 > 3$\sigma(F)$
(11) Molybdate	$P2_1/n$	915	0.0226	35 × 20 × 10	158	1.4	0.61 > 3$\sigma(I)$
(12) Lipid analogue	$P\bar{1}$	1105	0.0019	280 × 80 × 16	684	1.0	0.40 > 2$\sigma(I)$

(*d*) Further details of crystals

(1) $Au_{10}(PPh_3)_7[S_2C_2(CN)_2]_2$, synthesized as part of a general study of high nuclearity gold clusters, final R = 0.064 for 3747 reflections, F > 6$\sigma(F)$ (Cheetham, Harding, Haggitt, Mingos & Powell, 1993).

(2) $Al_3P_3O_{12}.nH_2O$ (*n ca* 5), synthetic aluminophosphate, supplied by L. B. McCusker; structure already known from powder diffraction (McCusker *et al.*, 1991), twinned crystal, final R = 0.075 for 289 reflections > 2$\sigma(I)$. This study confirmed the powder diffraction structure and gave some additional detail on water molecule sites (Cheetham & Harding, 1996).

(3) $Al_3(PO_4)_3F.C_4H_{10}NO$, a synthetic aluminophosphate, supplied by L. B. McCusker, final R = 0.081 for 289 reflections > 2$\sigma(I)$ (Harding & Kariuki, 1994).

(4) $C_{24}H_{40}O_4$, chenodeoxycholic acid, a low-temperature polymorph, final R = 0.11 for 578 reflections with F > 2$\sigma(F)$ (Rizkallah, Harding, Lindley, Aigner & Bauer, 1990).

(5) $(Cu,Zn)_5(OH)_6(CO_3)_2$, 5 μm thick flake of natural mineral, twinned crystal. Final R = 0.061 for 374 reflections, I > 2$\sigma(I)$ (Harding *et al.*, 1994).

(6) $Cu_2(OH)_2CO_3$ or $(Cu,Zn)_2(OH)_2CO_3$, very poor quality crystal from sample of mineral rosasite, final R = 0.12 for 153 reflections I > 2$\sigma(I)$ (Kariuki & Harding, 1995).

(7) $Mo_5O_{23}S_2.(NEt_4)_4.PhCN$, unexpected product of electrochemical synthesis, crystals from J. Iggo, final R = 0.107 for 2858 reflections I > 2$\sigma(I)$ (allowance not made for variation of f' and f'' with wavelength) (Maginn, Harding & Campbell, 1993).

(8) $C_{34}H_{26}N_2O_2$, organic pigment, crystal from W. Jones, two stereoisomers present with disorder (Kariuki & Harding, unpublished).

(9) $Rh_2H(PPh_2)(PPh_3)_4$, unexpected product in general study of rhodium organometallic compounds, supplied by G. Monks, final R = 0.094 for 3552 reflections, I > 3$\sigma(I)$ (not fully adjusted for variation of f' and f'' with wavelength) (Dodd, 1994).

(10) $(Y_{0.947}Dy_{0.078})PO_4.2H_2O$, natural mineral weinschenkite containing traces of other rare earths, final R = 0.077 for 637 reflections > 3$\sigma(F)$, λ = 1.00 Å, Hasylab (Kohlmann *et al.*, 1994).

(11) $NH_4(Mo_2P_2O_{10}).H_2O$, newly synthesized microporous material, λ = 0.915 Å, NSLS, Brookhaven National Laboratory, final R = 0.029 for 581 reflections > 3$\sigma(I)$ (King *et al.*, 1991).

(12) $(NH_4)^+.C_{18}H_{32}NO_6^-$, lipid model compound, λ = 0.46 Å, Doris, Hamburg, final R = 0.048 for 921 reflections > 2$\sigma(I)$ (Lehmann *et al.*, 1990).

† The true space group is shown in parentheses, but the scattering power and crystal volume refer to the primitive cell with half the volume.

from work in our own research group whereas the examples in (*c*) are taken from the published work of other research groups.

All the experiments were carried out with crystals which appeared to be the largest or best available for the material, and with the aim of establishing chemical constitution, connectivity and/or molecular geometry. Except for VPI-5, the structures were not previously known, and in each case knowledge of the structure was important to some major chemical research project. The structures were successfully determined, but in many cases the accuracy of the final structural information, the atom positions, interatomic distances, vibration parameters, was not comparable with that for a good structure refinement of a good-quality crystal. This is usually because the number of observed reflections falls far short of the number theoretically accessible; for many reflections the signal has been lost in the background [*i.e.* $I < 2\sigma(I)$ or some such criterion]. Even those reflections that are observed, with $I > 2\sigma(I)$, may not have intensity measurements as accurate as those in more favourable cases [*i.e.* have as large $I/\sigma(I)$]. A resolution [d_{min}, $(\lambda/2 \sin\theta)_{min}$] of at least 1 Å is desirable for structure determination and refinement. For all the above compounds the proportion of reflections observed to this limit, and the R factors achieved, are listed, as well as the scattering power. It should be borne in mind that many experiments were not performed with optimal conditions; if some data were lost due to beamtime shortage or equipment failures, but the structure could actually be established, the synchrotron radiation experiment has not normally been repeated. In this respect, working with synchrotron radiation is not like working in the home laboratory, where the experiment can

usually be continued until all the desired data are obtained. Many of the R factors are higher than those in current high-quality work; for the monochromatic data collections, probable explanations include the high proportion of weak reflections, poor and very variable spot shapes related to poor crystal quality, or inhomogeneity of the beam and beam movement.

One further example must be mentioned, the structure determination of $Mg_6(SO_2)(OH)_{14}$, published by Hamada *et al.* (1996) just as this article was otherwise complete. It exemplifies well both the possibilities and the problems. The crystals of this compound are extremely fine, long needles; the one selected was 0.5 × 100 × 2.5 μm, smaller than any of those listed in Table 2. Monochromatic image-plate data were recorded with Weissenberg geometry, for $k = 0, \pm 1$ at the Photon Factory (b is parallel to the needle axis), and the structure solved. The unit-cell scattering power, for comparison with Table 2, column 3, is $0.020\,e^2\,Å^{-6}$, and the fraction of unique reflections observed *ca* 0.30. From the spot shapes of this crystal and others in the sample it was evident that the crystals have some disorder in the direction perpendicular to the needle axis.

There are, in the literature, several accounts of diffraction experiments with crystallites appreciably smaller than those in Table 2(*a*), for example CaF_2 crystallites $(2.2)^3\,\mu m^3$ (Rieck, Euler, Schulz & Schildkamp, 1988), Mo spheres of diameter 0.8 μm (Ohsumi, Hagiya & Ohmasa, 1991), Bi crystallites of $0.038\,\mu m^3$ in metallic filaments (Skelton *et al.*, 1991). Their purposes have been quite different from structure determination and therefore they are not included in Table 2(*a*), although they provide useful examples of overcoming the problems of mounting, reducing background scatter *etc.*

8. Comparisons with powder diffraction

If large enough crystals for normal single-crystal structure determination methods are not available, powder diffraction methods are often considered. High-resolution powder diffraction patterns recorded with synchrotron radiation have allowed great advances in structure determination for materials of moderate complexity such as zeolites and aluminophosphates (McCusker, 1988, 1991). Of the structures in Table 2(*a*), that of VPI-5 (crystal 2) was determined by powder diffraction (McCusker, Baerlocher, Jahn & Bulow, 1991) before the single-crystal work was done. The single-crystal data served to confirm the low-symmetry space group, and to give more detail on the water molecule positions. The accuracy of the structure model refined with single-crystal data was a little better, but not much better, than that refined by the Rietveld method with the powder diffraction data, *i.e.* $\sigma_{\text{single crystal}}$ *ca* $0.5\sigma_{\text{powder}}$ for the Al, P and O positions. For $AlPO_4$-CHA (crystal 3, Table 2*a*), structure determination was achieved with powder data by McCusker & Simmen (Simmen, 1992) at about the same time as the single-crystal work; atom coordinates are in agreement, and in this case $\sigma_{\text{single crystal}}$ is approximately equal to σ_{powder}. Improvement in the accuracy of the single-crystal structures would have required the recording of a much larger number of independent reflection intensities, not achieved in either case.

Aurichalcite (crystal 5, Table 2*a*) was also examined by powder diffraction (Cernik, Bell & Cressey, 1994), but in this case structure solution was not achieved, probably because the presence of a substantial amount of impurity prevented the unit cell from being correctly identified, and the patterns indexed.

Even when the single crystals are small and their diffraction patterns weak, single-crystal methods have the advantage over powder diffraction data that unit-cell determination and indexing are much more straightforward, structure solution often so. In both cases the accuracy of the final structure obtained is limited by the amount of diffraction data that it is possible to record. With a single crystal this will decrease with the crystal size. The $AlPO_4$-CHA example seems to represent a borderline; with the experimental configuration available at the time, an even smaller crystal would have given fewer data, and refinement with the single-crystal data would have given less precise results than Rietveld refinement with the powder data.

The single-crystal data collections listed here have been carried out in substantially less beamtime than the corresponding powder diffraction time, *i.e.* 2–10 h each for those in Table 2(*a*), < 1 h each in Table 2(*b*) (where film change, safety protocols *etc.* take much more time than the actual exposures). On the other hand, occasionally, selecting one tiny single crystal from a 'powder' sample will yield an impurity crystal rather than one characteristic of the bulk sample (as probably happened with sample crystal 6 in Table 2*b*).

9. Crystal quality problems

It may appear paradoxical that we often found rather poor quality in very small crystals, whereas quite small crystals are intentionally selected for highly accurate studies of electron-density distributions; for example $YFeO_3$ crystals < 20 μm (du Boulay, Maslen, Streltsov & Ishizawa, 1995), or $CaCO_3$, $MgCO_3$ crystals < 30 μm (Maslen, Streltsov, Streltsova & Ishizawa, 1995) gave excellent diffraction data. These latter are of compounds from which good-quality large crystals can also be grown. However, when repeated attempts at crystallization fail to yield good-sized crystals, the small crystals often appear to be poor in quality; this may show as large mosaic spread, and there may be evidence of stacking faults. Although other factors may also influence crystal growth, it seems probable that the large mosaic spread and/or the existence of these faults is associated with the inhibition of growth. The evidence for this is explored in a little more detail below.

9.1. *Mosaic spread*

The effective mosaic spread represents the misalignment of mosaic blocks in an idealized model of a real crystal.

It is routinely evaluated in *MADNES* (Messerschmidt & Pflugrath, 1987) or other data-processing programs, since the size of the diffraction spots on the detector is determined by the mosaic spread, crystal size and the divergence of the incident beam. With our crystals, mosaic spread was the predominant contributor to spot size; values usually in the range 1–4° and occasionally up to 5 or 6° were found for the crystals in Table 2(*a*). Typical mosaic spreads for good-quality crystals, *e.g.* proteins, studied with synchrotron radiation are $\leq 0.1°$. The effect of mosaic spread on the size, or rocking width, of a diffraction spot, was illustrated in connection with the data collection and structure determination of a quite small crystal of piperazine silicate (Andrews *et al.*, 1988) and is shown in Fig. 3. Clearly, the large mosaic spread of these imperfect crystals makes the accurate measurement of reflection intensities much more difficult.

9.2. *Relationship to structure*

When data collection and structure determination have been achieved for these small crystals which do not grow larger, a structural explanation for poor growth or alignment can often be suggested. Morphology may be related to the growth problem: many small crystals are either very thin plates or very fine needles, which would be the result of inhibition of growth in one or two directions in the crystal. It is very commonly difficult to obtain large good crystals of aluminophosphates or zeolites; these compounds are characterized by pores or channels, *e.g.* 6–10 Å in diameter, through the structure; in crystal growth it would be understandable if the completion of the structure around each channel were subject to larger errors than the 'docking' of one fragment on a surface (or stepped surface) of a typical organic or inorganic crystal. In our limited experience very fine needle crystals correspond to structures with pores running in *one* direction in the crystal, parallel to the needle (*e.g.* VPI-5; crystal 2, Table 2*a*), whereas structures which have pores running in two directions yield crystals small in *all* dimensions, for example $AlPO_4$-CHA (crystal 3, Table 2*a*), SAPO-43 (Helliwell *et al.*, 1993). The crystals of cdc (crystal 4, Table 2*a*) are also very fine needles and in this structure too there are wide channels parallel to the needle axis (see Fig. 4). This structure consists of organic molecules, associated only by hydrogen bonds and van der Waals interactions, with poorly defined solvent molecules in the channels (in sharp contrast to the aluminophosphate structures where the framework of covalently bonded Al, P and O extends continuously in all directions).

The crystals of aurichalcite (crystal 5, Table 2*a*) are very thin flakes; this could be a simple result of the structure, which contains metal oxide layers with hydrogen bonds between. Poor growth in the direction perpendicular to the layers could also be related to local variations in the proportion of Zn and Cu atoms and to the effect this may have in inducing twinning (Harding, Kariuki, Cernik & Cressey, 1994).

In the organic pigment (crystal 8, Table 2*b*) the presence of two stereoisomers, disordered and in approximately equal proportions, in the crystal would certainly account for lack of perfection in the crystal packing, and perhaps the poor growth. It is a common observation, particularly in protein crystallography, that the presence of impurities reduces the likelihood of getting good-quality good-sized crystals.

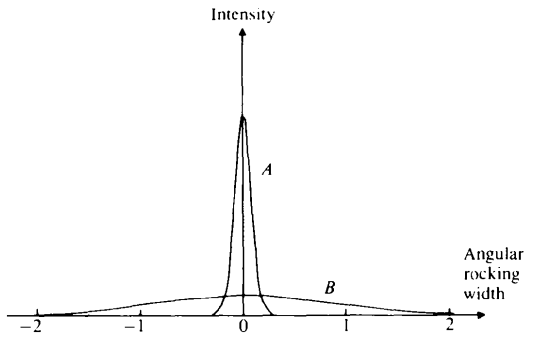

Figure 3
Effect of mosaic spread on the rocking width of a hypothetical crystal in a monochromatic diffraction experiment. The intensity of one reflection is shown as it would be recorded on an area detector while the crystal rotates through φ. For *A* the mosaic spread is 0.2° and for *B* it is 2°. The intensity, integrated over φ, is the same for both, but the problem of distinguishing signal from noise is much greater for *B*.

9.3. *Relationship between structure, mosaic spread and direction of limited growth*

The geometry of the Laue method is particularly sensitive to the mosaic spread. In an ideally imperfect crystal it will cause a Laue diffraction spot to be elongated radially, to a length of $2\eta D/\cos^2 2\theta$, where η is the mosaic spread and D the crystal detector distance (Andrews, Hails, Harding & Cruickshank, 1987). The elongation of the Laue diffraction spot also depends on the incident beam divergence, and the crystal or collimator dimensions (Helliwell *et al.*, 1988). Here, with synchrotron radiation beam divergence < 1 mrad, crystal dimensions < 0.2 mm, and substantial mosaic spread > 0.5°, the mosaic spread is the dominant effect; ignoring beam divergence and crystal size affects the predicted spot length by < 10%. For a crystal–detector distance of 60 mm, and θ *ca* 22° (near the edge of the patterns in typical experimental arrangements), $\eta = 0.5°$ should give spots of *ca* 2 mm in length, and $\eta = 1°$ spots of 4 mm.

In the idealized model it is assumed that the orientations of individual mosaic blocks are distributed over a range $\pm\eta/2$ about the mean *with equal probability*. If this were true the diffraction spots would have a sharply defined length and width. In real crystals the distribution may be roughly Gaussian, or in poor crystals more irregular than this. Spot length and width cannot be precisely defined, and depend on the spot intensity, background level *etc.* However, it is easy to make qualitative or semi-quantitative comparisons of mosaic spread in different crystals. In some

cases it is also clear that spot lengths, and thus mosaic spread, are different for reflections in different regions of the reciprocal lattice of one crystal. Fig. 5(*a*) shows a Laue diffraction pattern of a crystal of cdc (crystal 4, Table 2*a*), whose structure has been described above and illustrated in Fig. 4; Fig. 5(*b*) indicates the indices of some of the reflections on the image. The radial extension of spots is greatest near the a^*b^* plane of the reciprocal lattice where it corresponds to a mosaic spread of 0.8–1°; in directions near c^* the spots are much shorter and sharper, corresponding to a mosaic spread < 0.2°. So in this case it is shown that the direction of poor growth (or at least of very small crystal dimensions) corresponds to the direction with large mosaic spread, whereas the larger dimension, the needle axis, corresponds to the direction of smaller mosaic spread. Very similar conclusions were drawn for a

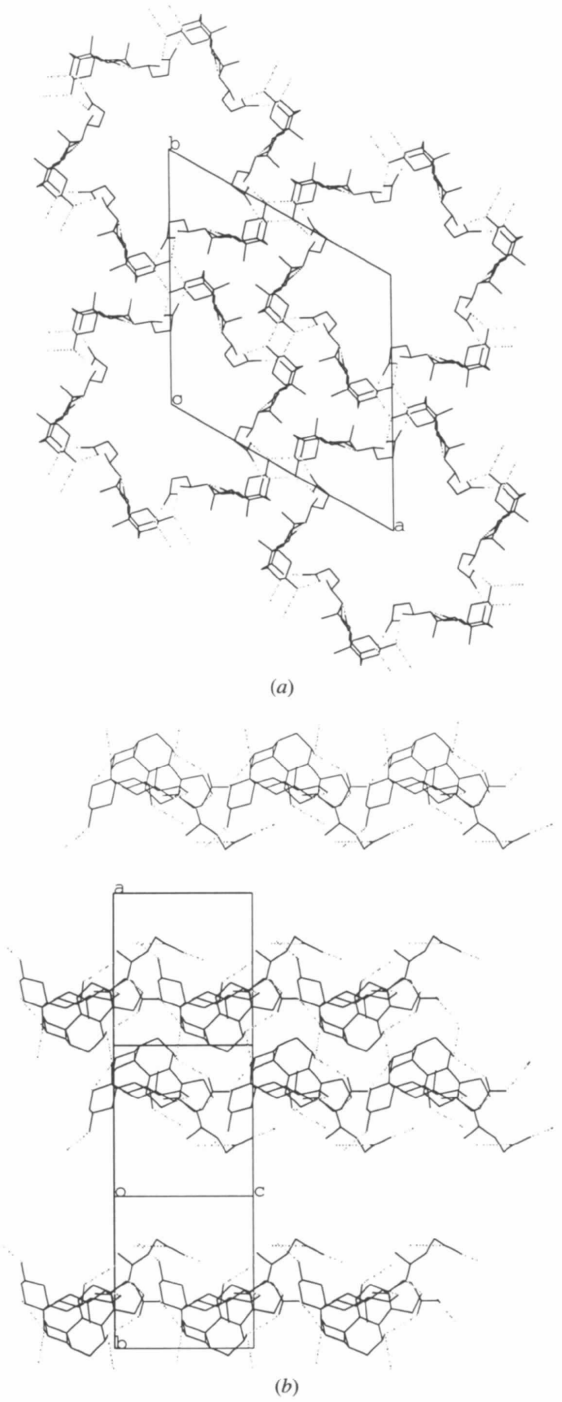

(*a*) (*b*)

Figure 4
Channels in the structure of chenodeoxycholic acid (crystal 4, Table 2*a*). (*a*) *c*-axis view of whole structure, (*b*) *b*-axis view, including only molecules with $-1/4 < y < 1/4$; dotted lines show hydrogen bonds.

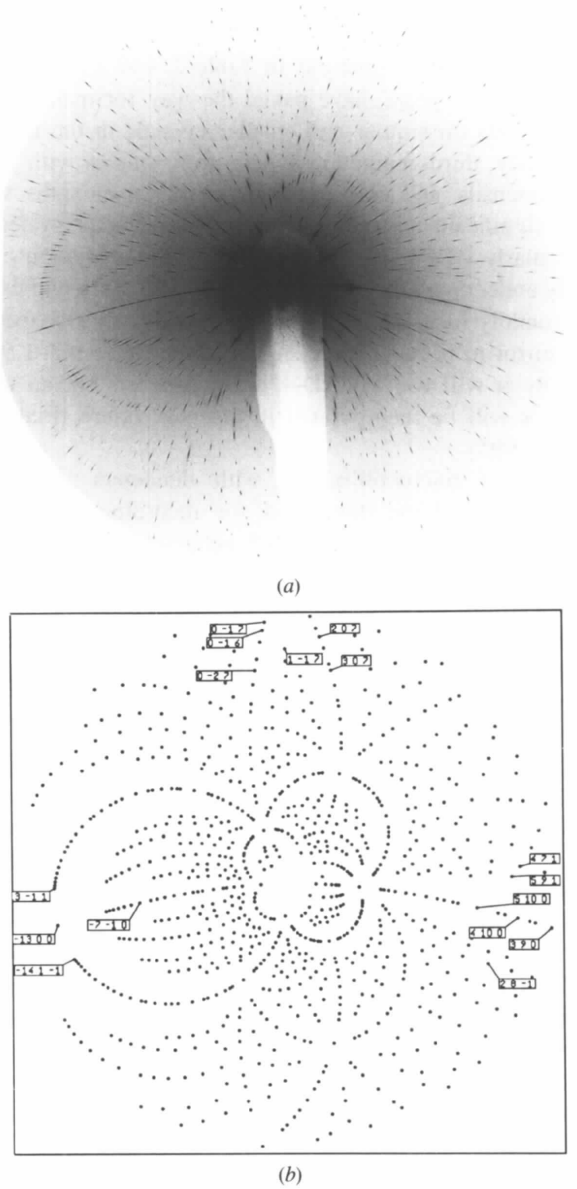

(*a*) (*b*)

Figure 5
(*a*) Laue diffraction pattern of chenodeoxycholic acid (crystal 4, Table 2*a*), recorded on film at Daresbury Laboratory on workstation 9.7. (*b*) Simulation of the Laue diffraction pattern, with indices shown for a small selection of reflections. (The crystal has a = 22.25, c = 10.255 Å, space group $P6_5$, and the predicted Laue image assumes λ_{min} = 0.25, λ_{max} = 2.0, d_{min} = 1.4 Å, crystal–film distance = 60 mm.)

crystallite of the Si-doped aluminophosphate SAPO-5. The structure was determined from monochromatic synchrotron radiation diffraction data for a hexagonal needle crystal of dimensions 30 × 15 × 180 μm (Rizkallah, Harding & Kaucic, 1990). It was shown to be hexagonal, of the APO-5 type (Meier & Olson, 1987), with channels parallel to *c* and *ca* 8 Å across, but Si atoms could not be distinguished from P or Al atoms. Laue diffraction patterns were recorded and examined by Rule (1990), and the mosaic spread shown to be substantially larger in directions perpendicular to the needle axis than parallel to it.

10. Conclusions – the future

The structure determinations in Table 2, and a few others in the last ten years, have paved the way for many more experiments on similar and smaller crystals in the future. Obviously, third-generation synchrotron sources with very high intensity and comparatively short wavelengths will be a significant advantage. Newer area-detector systems, particularly CCDs, will be important. A workstation currently under construction at Daresbury Laboratory will use a horizontally focusing monochromator and vertically focusing mirror to provide wavelengths in the range 0.3–1.5 Å; initially it will use a CAD-4 diffractometer, but an area detector will be incorporated in the near future (Flaherty *et al.*, 1995).

Capillary microcollimators with diameters less than 10 μm have been developed for recording diffraction patterns of very small selected areas of polycrystalline or other samples (Bilderback, Hoffman & Thiel, 1994; Riekel & Engstrom, 1995; Mahendrasingam *et al.*, 1995). Hirano & Usami (1994) have used focusing and slits to produce an X-ray beam of dimensions 6 × 8 μm, again for the study of selected areas of a larger sample. The use of smaller collimators, for example 20, 50 or 100 μm in diameter, would be a big advantage. Development work on microcollimators and microcapillary collimators, some of which concentrate the beam, is also described by Bilderback, Thiel, Pahl & Brister (1994) and Thiel, Bilderback, Lewis & Stern (1992). The use of such small collimators will, in turn, place high demands on the mechanical accuracy and stability of alignment systems for the collimator and the crystal rotation axis or axes. Some further reduction of background might be possible using a helium enclosure, and crystal cooling to near liquid-nitrogen temperatures should give a modest further improvement in the discrimination of spot from background.

Technical improvements such as these should make possible the study of smaller crystals, *e.g.* aluminophosphates down to 1–5 μm in dimensions. Caution will be needed in the interpretation of intensity measurements, as Neder (1995) has pointed out, when the volume fraction of the near-surface atoms becomes appreciable, perhaps for dimensions *ca* 0.1 μm. There will remain the challenge of the unpredictable, often poor quality of these small crystals.

I am grateful to EPSRC for financial support, to Daresbury Laboratory for synchrotron radiation facilities, and for the cooperation and support of many staff there, from whom I have learned so much. I am also grateful to Dr Benson Kariuki, Dr R. J. Rule and others who worked with me at Liverpool University, to Professor John Helliwell (University of Manchester) for advice and help over many years, and to the late Dr Barrie Lowe (University of Edinburgh) for interesting discussions on the growth and structure of small crystals.

References

Allinson, N. M. (1994). *J. Synchrotron Rad.* **1**, 54–62.
Andrews, S. J., Hails, J. M., Harding, M. M. & Cruickshank, D. W. J. (1987). *Acta Cryst.* A**43**, 70–73.
Andrews, S. J., Papiz, M. Z., McMeeking, R. M., Blake, A. J., Lowe, B. M., Franklin, K. R., Helliwell, J. R. & Harding, M. M. (1988). *Acta Cryst.* B**44**, 73–77.
Arndt, U. W. (1990). *Synchrotron Rad. News*, **3**, 17–22.
Bilderback, D. H., Hoffman, S. A. & Thiel, D. J. (1994). *Science*, **263**, 201–293.
Bilderback, D. H., Thiel, D. J., Pahl, R. & Brister, K. E. (1994). *J. Synchrotron Rad.* **1**, 37–42.
Boulay, D. du, Maslen, E. N., Streltsov, V. A. & Ishizawa, N. (1995). *Acta Cryst.* B**51**, 921–929.
Carr, P. D., Cruickshank, D. W. J. & Harding, M. M. (1992). *J. Appl. Cryst.* **25**, 294–308.
Carr, P. D., Dodd, I. M. & Harding, M. M. (1993). *J. Appl. Cryst.* **26**, 384–387.
Cassetta, A., Deacon, A., Emmerich, C., Habash. J., Helliwell, J. R., McSweeney, S., Snell, E., Thompson, A. W. & Weisgerber, S. (1993). *Proc. R. Soc. London Ser. A*, **442**, 177–192.
Cernik, R., Bell, A. & Cressey, G. (1994). Personal communication.
Cheetham, G. M. T. & Harding, M. M. (1996). *Zeolites*, **16**, 245–248.
Cheetham, G. M. T., Harding, M. M., Haggitt, J. L., Mingos, D. M. P. & Powell, H. R. (1993). *J. Chem. Soc. Chem. Commun.* pp. 1000–1001.
Deacon, A., Habash, J., Harrop, S. J., Helliwell, J. R., Hunter, N. W., Leonard, G. A., Peterson, M., Hadener, A., Kalb, A. J., Allinson, N. M., Castelli, C., Moon, K., McSweeney, S., Gonzalez, A., Thompson, A., Ealick, S., Szebenyi, D. M. & Walter, R. (1995). *Rev. Sci. Instrum.* **66**, 1287–1292.
Dodd, I. M. (1994). PhD thesis, University of Liverpool, UK.
Dodd, I. M., Hao, Q., Harding, M. M. & Prince, S. M. (1994). *Acta Cryst.* B**50**, 441–447.
Flaherty, J. V., Burrows, I., Irvin, P., Clegg, W., Catlow, C. R. A., Cernik, R. J., Greaves, G. N. & Bushnell-Wye, G. (1995). *Annual Report for 1994–1995*, pp. 362–363, Synchrotron Radiation Department, CCLRC Daresbury Laboratory, Warrington WA4 4AD, UK.
Hamada, E., Ishizawa, N., Marumo, F., Ohsumi, K., Shimizugawa, Y., Reizen, K. & Matsunami, T. (1996). *Acta Cryst.* B**52**, 266–269.
Harding, M. M. (1991). *J. Phys. Chem. Solids*, **52**, 1293–1298.
Harding, M. M. (1995). *Acta Cryst.* B**51**, 432–446.
Harding, M. M. & Kariuki, B. M. (1994). *Acta Cryst.* C**50**, 852–854.
Harding, M. M., Kariuki, B. M., Cernik, R. & Cressey, G. (1994). *Acta Cryst.* B**50**, 673–676.
Helliwell, J. R. (1992). *Macromolecular Crystallography with Synchrotron Radiation*. Cambridge University Press.

Helliwell, J. R., Ealick, S., Doing, P., Irving, T. & Szebenyi, D. M. (1993). *Acta Cryst.* D**49**, 120–128.
Helliwell, J. R., Habash, J., Cruickshank, D. W. J., Harding, M. M., Greenhough, T. J., Campbell, J. W., Clifton, I. J., Elder, M., Machin, P. A., Papiz, M. Z. & Zurek, S. (1988). Daresbury Laboratory Preprint DL/SVCI/P588E. CCLRC Daresbury Laboratory, Warrington WA4 4AD, UK.
Helliwell, J. R., Habash, J., Cruickshank, D. W. J., Harding, M. M., Greenhough, T. J., Campbell, J. W., Clifton, I. J., Elder, M., Machin, P. A., Papiz, M. Z. & Zurek, S. (1989). *J. Appl. Cryst.* **22**, 483–497.
Helliwell, M., Kaucic, V., Cheetham, G. M. T., Harding, M. M., Kariuki, B. M. & Rizkallah, P. J. (1993). *Acta Cryst.* B**49**, 413–420.
Helliwell, J. R., Papiz, M. Z., Glover, I. D., Habash, J., Thompson, A. W., Moore, P. R., Harris, N., Croft, D. & Pantos, E. (1986). *Nucl. Instrum. Methods*, A**246**, 617–623.
Hirano, T. & Usami, K. (1994). *J. Mater. Res.* **9**, 112–115.
Kariuki, B. M. & Harding, M. M. (1995). *J. Synchrotron Rad.* **2**, 185–189.
King, H. E., Mundi, L. A., Strohmaier, K. G. & Haushalter, R. C. (1991). *J. Solid State Chem.* **92**, 1–7.
Kohlmann, M., Sowa, H., Reithmayer, K. & Schulz, H. (1994). *Acta Cryst.* C**50**, 1651–1652.
Krumrey, M., Kvick, A. & Schwegle, W. (1995). *Rev. Sci. Instrum.* **66**, 1715–1717.
Lehmann, C. W., Buschmann, J., Luger, P., Demoulin, C., Fuhrhop, J. H. & Eichorn, K. (1990). *Acta Cryst.* B**46**, 646–650.
McCusker, L. B. (1988). *J. Appl. Cryst.* **21**, 305–310.
McCusker, L. B. (1991). *Acta Cryst.* A**47**, 297–313.
McCusker, L. B., Baerlocher, C., Jahn, E. & Bulow, M. (1991). *Zeolites*, **11**, 308–313.
Maginn, S. J., Harding, M. M. & Campbell, J. W. (1993). *Acta Cryst.* B**49**, 520–524.
Mahendrasingam, A., Martin, C., Fuller, W., Blundell, D. J., Mackerron, D., Rule, R. J., Oldman, R. J., Liggat, J., Riekel, C. & Engstrom, P. (1995). *J. Synchrotron Rad.* **2**, 308–311.
Maslen, E. N., Streltsov, V. A., Streltsova, N. R. & Ishizawa, N. (1995). *Acta Cryst.* B**51**, 929–939.
Meier, W. M. & Olson, D. H. (1987). *Atlas of Zeolite Structure Types*, p. 18. London: Butterworth.
Messerschmidt, A. & Pflugrath, J. W. (1987). *J. Appl. Cryst.* **20**, 306–315.
Neder, R. B. (1995). *Z. Kristallogr.* **210**, 415–417.
Ohsumi, K., Hagiya, K. & Ohmasa, M. (1991). *J. Appl. Cryst.* **24**, 340–348.
Rieck, W., Euler, H., Schulz, H. & Schildkamp, W. (1988). *Acta Cryst.* A**44**, 1099–1101.
Riekel, C. & Engstrom, P. (1995). *Nucl. Instrum. Methods*, B**97**, 224–230.
Rizkallah, P. J., Harding, M. M. & Kaucic, V. (1990). Unpublished.
Rizkallah, P. J. Harding, M. M., Lindley, P. F., Aigner, A. & Bauer, A. (1990). *Acta Cryst.* B**46**, 262–266.
Rule, R. J. (1990). PhD thesis, University of Liverpool, UK.
Simmen, A. (1992). PhD thesis, ETH, Zurich, Switzerland.
Skelton, E. F., Ayers, J. D., Quadri, S. B., Moulton, N. E., Cooper, K. P., Finger, L. W., Mao, H. K. & Hu, Z. (1991). *Science*, **253**, 1123–1125.
Snell, E., Habash, J., Helliwell, M., Helliwell, J. R., Raftery, J., Kaucic, V. & Campbell, J. W. (1995). *J. Synchrotron Rad.* **2**, 22–26.
Thiel, D. J., Bilderback, D. H., Lewis, A. & Stern, E. A. (1992). *Nucl. Instrum. Methods*, A**317**, 597–600.